Article

Effect of Cooling Rates on the Microstructure and Mechanical Property of La Modified Al7SiMg Alloys Processed by Gravity Die Casting and Semi-Solid Die Casting

Longfei Li [1,2], Daquan Li [1,*], Jian Feng [1], Yongzhong Zhang [1] and Yonglin Kang [2]

[1] General Research Institute for Nonferrous Metals, Beijing 100088, China; lilongfei_grinm@163.com (L.L.); fengjian427@126.com (J.F.); yyzhang@grinm.com (Y.Z.)

[2] School of Materials Science and Engineering, University of Science and Technology Beijing, Beijing 100083, China; kangylin@ustb.edu.cn

[*] Correspondence: lidaquan@grinm.com; Tel.: +86-010-6066-2681

check for updates

Abstract: Rare earth (RE) additions are capable of refining the α-Al phase as well as modifying the eutectic Si particles of alloys. The cooling rate in casting process should be carefully concerned when the Al-Si alloys are refined and modified by adding RE elements. In this study, the effect of cooling rates on the microstructure and mechanical properties of La modified Al-7.0Si-0.3Mg alloys was studied in gravity die casting and semi-solid die casting. It is found that in La modified Al-7.0Si-0.3Mg alloys, with increasing the cooling rate from 0.2 to 9 K/s in gravity die casting, the α-Al grains are greatly refined and the Si particles are modified to branching morphology, which evidently increases the UTS and elongation of alloys. In addition, when increasing the cooling rate from 30 to 130 K/s in semi-solid die casting, the α-Al grains are refined from 140 to 47 μm, and the Si particles are modified to fibrous morphology, which increases the UTS from 190 to 230 MPa and elongation from 10% to 11%. However, the 0.4 wt.% La addition results to La-rich phases formed in microstructure, which impairs the mechanical properties of Al-7.0Si-0.3Mg alloys in semi-solid die casting.

Keywords: Al-Si alloys; cooling rate; rare earth La; microstructure; mechanical property

1. Introduction

The Al-Si-Mg alloys, which owe excellent casting characteristics including good fluidity and less solidification shrinkage [1,2], are broadly applied in casting industry [3–5]. However, in a normal casting process, the α-Al grains have coarse dendritic morphology, and the Si particles generally have acicular morphology and discontinuous distribution, which have detrimental influence on the strength and especially elongation of the aluminum alloys [6,7]. The chemical refinement and modification, which is achieved by adding small amount modifying elements (Ti, Sr, rare earth), is a useful method to refine the α-Al grains and improve the Si morphology, and therefore enhance the mechanical properties of alloys [8–10]. Currently, the RE elements, which are able to refine the α-Al grains and form the flake-to-fiber transition in eutectic Si, are extensively studied in Al-Si-Mg alloys. Kang et al. [11] found the synergistic addition of Ce (0.1 wt.%) and Mg (0.7 wt.%) not only has an obvious refining effect on α-Al grains but also modifies the eutectic Si to fibrous morphology. Emamy [12,13] studied the effect of La addition in A357 alloys and pointed out the optimum amount of La (0.1 wt.%) decreases the grain size to 50% and changes the Si particles from irregular to fine fiber-like morphology. Jiang et al. [14] investigated the influence of Ce and La additions on the microstructure of A357 alloys, and found the

reduction of grain size and second dendrite arm spacing (SDAS) of α-Al are 48.1% and 162.2%, and that the aspect ratio of Si particles decreases by 142%.

For eutectic Si modified by RE elements, it is accepted that the modification effect has a close relationship with the cooling condition in casting process. Mao et al. [15] pointed out different modification mechanisms exist in hypoeutectic Al-Si alloys modified with yttrium (Y) in different cooling rates. Liu et al. [16] investigated the microstructural evolution of Si in Al-Si alloys modified with Ce-rich mischmetal at different cooling rates and concluded that effective modification is obtained by a combination of the RE elements and rapid cooling rate. Therefore, the cooling condition in casting process should be carefully concerned while adding RE elements.

In this study, the microstructures and mechanical properties of Al-7.0Si-0.3Mg alloys modified by 0.4 wt.% La addition are studied in gravity die casting and semi-solid die casting. The α-Al grains, eutectic Si and La-rich phases in Al-7.0Si-0.3Mg without and with 0.4 wt.% La are evaluated with increased cooling rates during solidification. The relationship between the microstructure and mechanical properties of the alloys is also discussed in two casting processes.

2. Materials and Methods

Al-7 wt.%Si-0.3 wt.%Mg (hereafter denoted as Al7SiMg) alloys containing 0.4 wt.% La were prepared from commercial-purity Al, Mg, Si, and Al-20 wt.% La alloys. The compositions of alloys used in experiment are listed in Table 1. The content of La element was analyzed by inductively coupled plasma atomic emission spectrometry (ICP-AES) apparatus. After loading the pure Al, Si into clay-graphite crucible, the electric resistance furnace was setting to 730 °C. When the alloys were melted, the pure Mg was gently pressed into melt using an iron cover to avoid burning loss. The Al-20 wt.% La alloys were added when the melt was homogenized at 730 °C. A graphite pipe with argon was used to remove dissolved hydrogen in melt. After degassing for 20 min, the melt was held for 20 min and then skimmed to remove the impurities on the melt surface.

Table 1. Composition of Al7SiMg and Al7SiMg + 0.4La. (weight percent).

Alloy	Si	Mg	La	Ti	Sr	Others	Al
Al-7Si-0.3Mg	7.05	0.368	<0.01	<0.0002	<0.0001	<0.10	Bal.
Al-7Si-0.3Mg-0.4La	6.96	0.349	0.38	<0.0002	<0.0001	<0.10	Bal.

In this study, two processes including the gravity die casting and semi-solid die casting are applied. Figure 1 is the schematics of crucible and castings used in gravity die casting. The pouring temperature of melt was chosen to 730 °C and the pre-heated temperature of the mold was optimized to 300 °C. The cooling curves during pouring and solidification have been measured by using USB-2416 multifunction temperature device (MC Measurement Computing, Measurement Computing Corporation, Norton, MA, USA). A previous study [17] shows that the cooling rate between the interval of 580 °C~600 °C for three molds were 0.2, 1.5, and 9 K/s, respectively.

The semi-solid die casting process includes the semi-solid slurry preparation and high pressure die casting. In this study, the SEED (Swirling Enthalpy Equilibrium Device) method, which has been into industrial and commercial stages [18], was used to make semi-solid slurry with 50% solid fraction. During the die casting process, a plunger of velocity of 0.1 m s^{-1} and intensity pressure of 90 MPa were chosen to obtain complete castings with less shrinkage porosity. Figure 2 shows the schematics of castings used in semi-solid die casting process. Due to much difficulty in measuring the cooling rate during high pressure die casting process, the ProCast software (version 2016, ESI group, Paris, France) was used to evaluate the cooling rate of sampling points. The estimated cooling rates of two molds with thickness of 30 and 0.8 mm were 30 and 130 K/s, respectively.
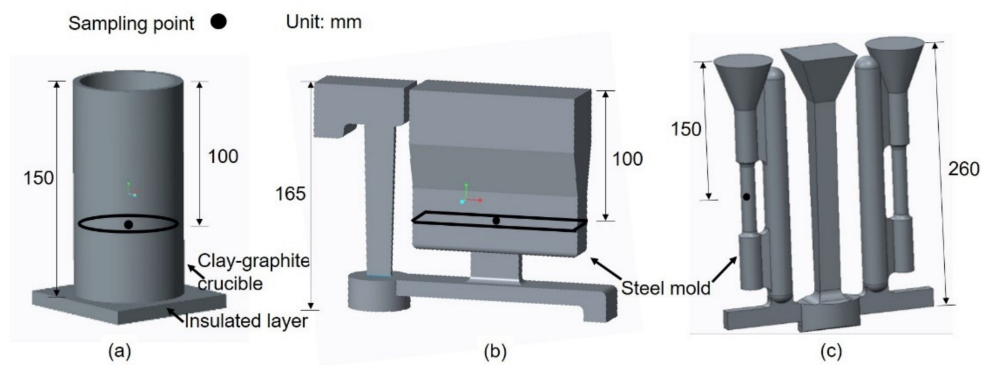
Figure 1. Schematic diagram of (**a**) clay-graphite crucible, (**b**) castings for self-design permanent mold, and (**c**) castings for ASTM B-108 permanent mold used in gravity die casting.
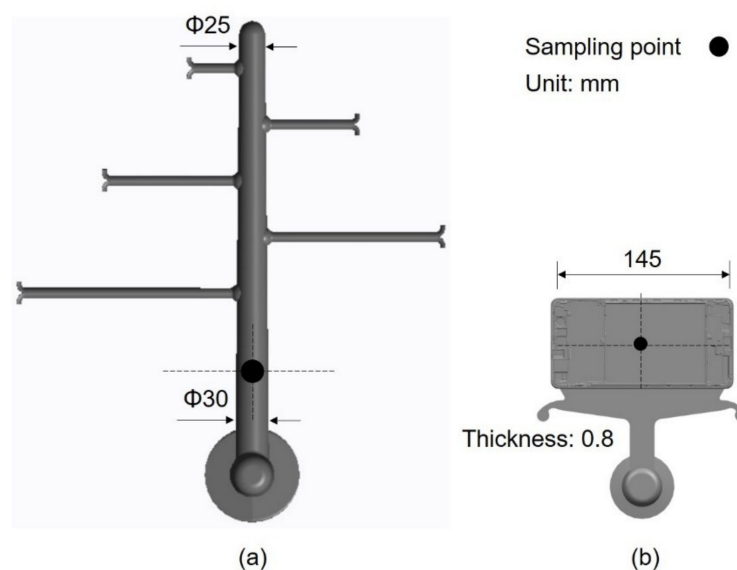
Figure 2. Schematic diagram of castings with (**a**) thick-wall for 30 mm thickness and (**b**) thin-wall for 0.8 mm thickness in semi-solid die casting.

The samples for Optical Microscope (OM) observation were mechanically ground using 80, 240, 600, 800, 1500, and 2000 grits' sandpapers, and were then polished using 3.5 and 1.5 grits' paste. The α-Al grains were anodized by using Baker reagent, which has a concentration of 5 g HBF_4 acid in 100 mL H_2O. The transversal method (ASTM E112) was used to measure the size of α-Al grain. The samples were etched using 20 vol.% HF solution for 20 min to show the three-dimension (3D) morphology of eutectic Si. The 3D morphology of eutectic Si and the La-rich phases in microstructure were observed using the Field Emission Scanning Electron Microscope (FESEM, JSM-7610-plus, JEOL Ltd., Tokyo, Japan) equipped with energy dispersive spectroscopy (EDS).

To compare the mechanical properties of alloys in different cooling rates, the tensile test bars in each group were machined in the vicinity of sampling points and key dimensions are shown in Figure 3. At the cooling rate of 0.2, 1.5, 9, and 30 K/s, the circular tensile specimens were machined, and key dimensions can be seen in Figure 3a. The thin plate specimens were machined at the cooling rate of 130 K/s and the key dimensions are shown in Figure 3b. The tensile tests were performed with an Instron 5500 Universal Electromechanical Testing System (INSTRON Ltd., Norwood, MA, USA). The strain rate during tensile tests was within $10^{-4} \sim 10^{-3}$ s^{-1}. Three tensile specimens were tested to get the reported mechanical properties.
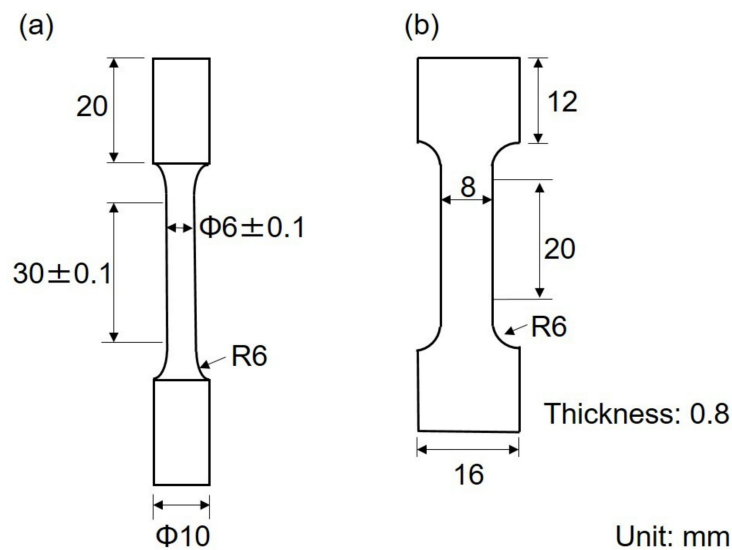
Figure 3. Key dimensions of the (**a**) circular tensile specimen and (**b**) thin plate specimen.

3. Results

3.1. Effect of Cooling Rates in Gravity Die Casting

In Figure 4, the microstructures in polarized light of α-Al grains in Al7SiMg alloys without and with 0.4 wt.% La are displayed at the cooling rate of 0.2, 1.5, and 9 K/s. It is obvious that the refining effect is produced with La additions, the α-Al grains have smaller dendrite arm spacing (DAS) and grain size with increasing cooling rates. Figure 5 is the measurement of DAS and grain size of α-Al grains in alloys at different cooling rates. When the cooling rate increases from 0.2 to 9 K/s, the DAS of α-Al grains in Al7SiMg alloys decreases from 106 to 19 μm, and the DAS of α-Al grains in Al7SiMg alloys with 0.4 wt.% La decreases from 99.1 to 21 μm. In Figure 5b, for Al7SiMg alloys, it is shown that the grain size decreases from 1321 to 485 μm when increasing the cooling from 0.2 to 9 K/s. For Al7SiMg alloys containing 0.4 wt.% La, when the cooling rate increases from 0.2 to 9 K/s, the average grain size decreases from 738 to 353 μm. It is concluded that the grain size and DAS of the α-Al phase are significantly decreased with increasing cooling rate. In addition, the 0.4 wt.% La addition has an obvious refining effect on the α-Al grains at the cooling rate of 0.2, 1.5, and 9 K/s.
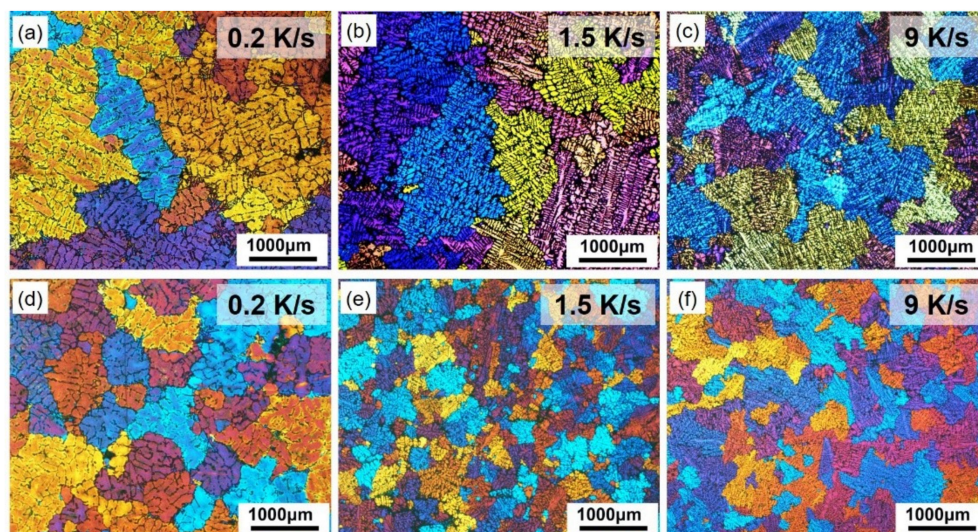
Figure 4. Microstructure in polarized light showing the α-Al grains of (**a**–**c**) Al7SiMg and (**d**–**f**) Al7SiMg + 0.4La alloys in different cooling rates.
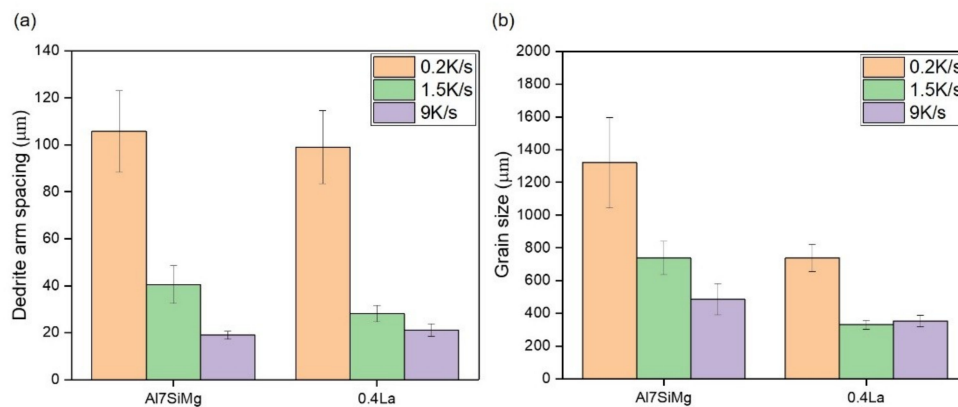
Figure 5. Measurement of (**a**) DAS and (**b**) grain size of α-Al grains in Al7SiMg alloys without and with 0.4 wt.% La at different cooling rates.

The 3D morphology of eutectic Si at different cooling rates is shown in Figure 6. For Al7SiMg alloys (Figure 6a–c), the Si particles show flake-like morphology and grow in planar mode. For Al7SiMg alloys with 0.4 wt.% La addition, at the cooling rate of 0.2 K/s (Figure 6d), the eutectic Si particles have coarse flake-like morphology, with increasing the cooling rate to 9 K/s (Figure 6f), the Si particles have a branching morphology and display in continuous distribution. At higher cooling rate, the Si modification effect is greatly increased when the Al7SiMg alloys are modified with 0.4 wt.% La.
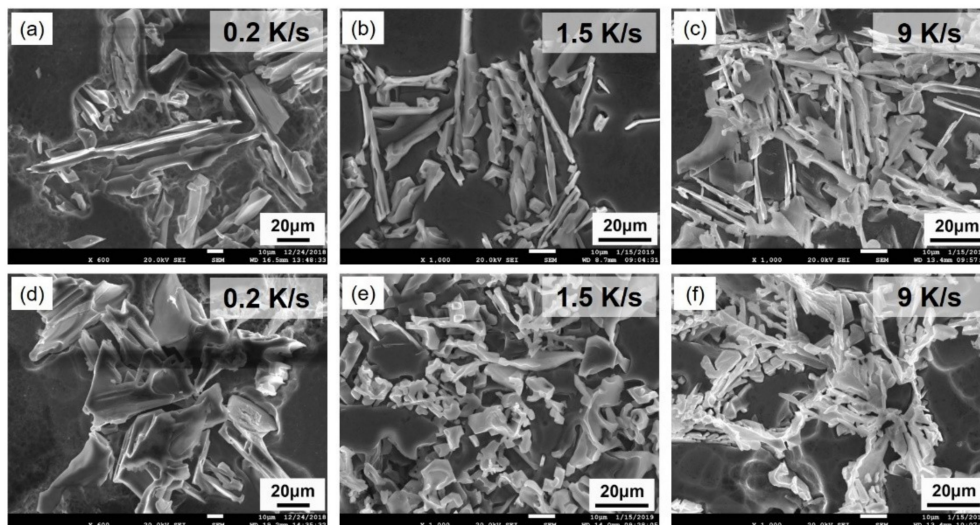
Figure 6. The 3D morphology of eutectic Si in (**a**–**c**) Al7SiMg and (**d**–**f**) Al7SiMg+0.4La alloys at different cooling rates.

The microstructures of La-rich phases are shown in Figure 7. It can be observed that, at the cooling rate of 0.2 K/s, the coarse La-rich phases precipitate in the grain boundaries. As shown in magnified microstructure in Figure 7a, some La-rich phases are present in irregular shape. When increasing the cooling rate to 1.5 and 9 K/s, the La-rich phases in short rod shape are observed in microstructure (Figure 7b,c). It is also observed the number of La-rich phases per unit area is increased with increasing cooling rates—the higher cooling rate in semi-solid die casting can confirm this observation.
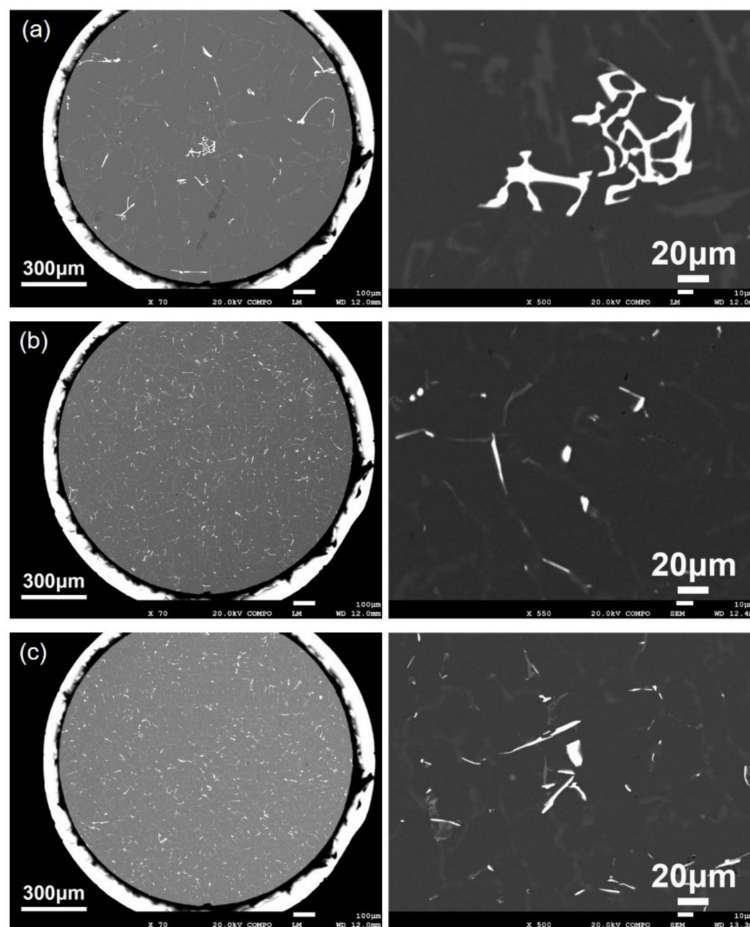
Figure 7. SEM microstructure showing the morphology of La-rich phases. (**a**) 0.2, (**b**) 1.5, (**c**) 9 K/s.

The tensile properties are outlined in Table 2. For Al7SiMg alloys, with increasing cooling rate, the UTS has an obvious increase, while the elongation of alloys shows no much influence. The addition of La enhances the UTS and elongation under higher cooling rates (1.5 and 9 K/s). At the cooling rate of 0.2 K/s, the UTS and elongation of Al7SiMg are 140 MPa and 2.2%, respectively. The alloys containing 0.4 wt.% La have UTS of 140 MPa, elongation of 2.5%. With increasing the cooling rate to 9 K/s, the UTS of alloys without and with 0.4 wt.% La are 160 MPa and 180 MPa, and the elongation of alloys without and with 0.4 wt.% La are 2.1% and 4.6%, respectively.

Table 2. Tensile properties of Al7SiMg and Al7SiMg + 0.4La alloys at different cooling rates. (YS = yield strength, UTS = ultimate tensile strength, EL = elongation).

Cooling Rate (K/s)	Alloys	YS (MPa)	UTS (MPa)	EL (%)
0.2 K/s	Al7SiMg	93 ± 2.9	140 ± 0.5	2.2 ± 0.1
	0.4 La	94 ± 3.7	140 ± 0.5	2.5 ± 0.1
1.5 K/s	Al7SiMg	85 ± 1.9	130 ± 13	2.1 ± 0.8
	0.4 La	89 ± 2.8	160 ± 6.0	3.2 ± 0.7
9 K/s	Al7SiMg	95 ± 5.2	160 ± 13	2.1 ± 0.6
	0.4 La	91 ± 3.3	180 ± 4.2	4.6 ± 0.1

Figure 8 is the SEM pictures showing the fracture morphology of Al7SiMg alloys without and with 0.4 wt.% La at the cooling rate of 0.2 and 9 K/s. For Al7SiMg alloys, the flat cleavage planes and tears ridges in straight line shape are observed at the cooling rate of 0.2 K/s (Figure 8a), which indicates a brittle fracture. In Figure 8b, with increasing the cooling rate to 9 K/s, the curved tear ridges are obtained. When the 0.4 wt.% La is added to the base alloys, as shown in Figure 8c, the brittle fracture mode is obtained at the cooling rate of 0.2 K/s. When the cooling rate is 9 K/s, more dimples are observed on the fracture (Figure 8d). This shows the ductility is enhanced by La additions at a higher cooling rate.
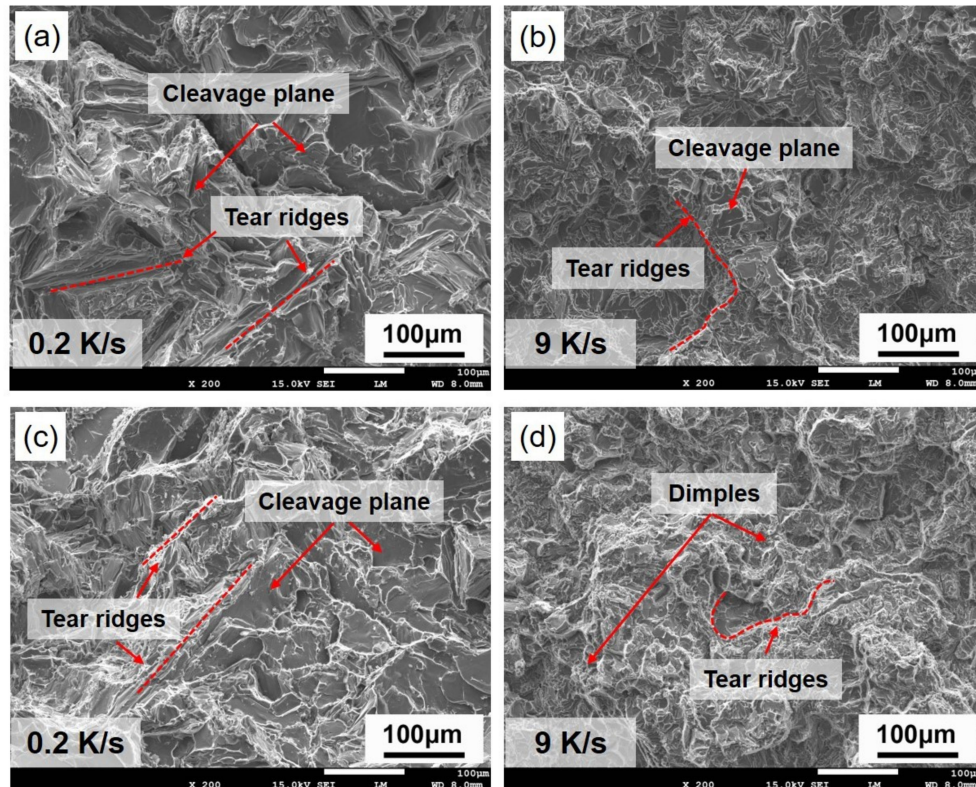
Figure 8. SEM pictures showing the fractures of (**a**,**b**) Al7SiMg and (**c**,**d**) Al7SiMg+0.4La at the cooling rate of 0.2 and 9 K/s.

3.2. Effect of Cooling Rates in Semi-Solid Die Casting

Figure 9 is the microstructure of α-Al grains at the cooling rate of 30 and 130 K/s. In the semi-solid die casting process, the α-Al grains show the globular morphology. The measurement of α-Al grains size is shown in Figure 10. When the cooling rate is 30 and 130 K/s, the grain sizes of Al7SiMg alloy are 133 and 44 μm, and the grain sizes of La modified alloys are 140 and 47 μm. Similar to the condition in the gravity die casting, the α-Al grains are greatly refined with increasing cooling rate. However, it is obtained the addition of 0.4 wt.% La has no refining effect on globular α-Al grain in the semi-solid die casting.

The 3D morphology of eutectic Si and magnified pictures at the cooling rate of 30 and 130 K/s are shown in Figure 11. For Al7SiMg alloys (Figure 11a), the eutectic Si shows flake-like morphology and has noticeable growth planes at the cooling rate of 30 K/s. Increasing the cooling rate to 130 K/s, the eutectic Si has a well branching structure, and some Si rods grow vertically to the irregular Si planes, which is highlighted by the red arrow in Figure 11b. Under the condition of 0.4 wt.% La addition, the Si particles with fiber-like morphology are obtained at the cooling rate of 30 K/s (Figure 11c). When the cooling rate is 130 K/s (Figure 11d), a better modification effect is obtained, and the eutectic Si particles show a very fine and nodular morphology. It is obvious the high cooling rate enhances the Si

modification effect in the alloys without and with La addition. Moreover, the modification effect of 0.4 wt.% La is furtherly enhanced with increasing cooling rate.
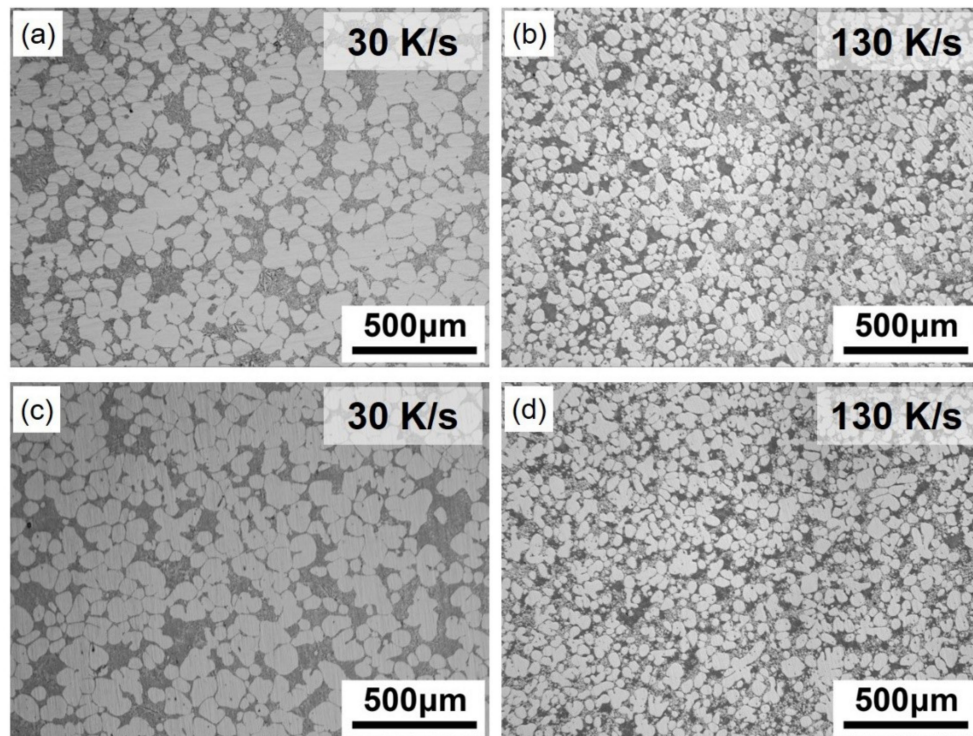
Figure 9. Microstructure showing the α-Al grains in (**a**,**b**) Al7SiMg and (**c**,**d**) Al7SiMg + 0.4La alloys at the cooling rate of 30 and 130 K/s.
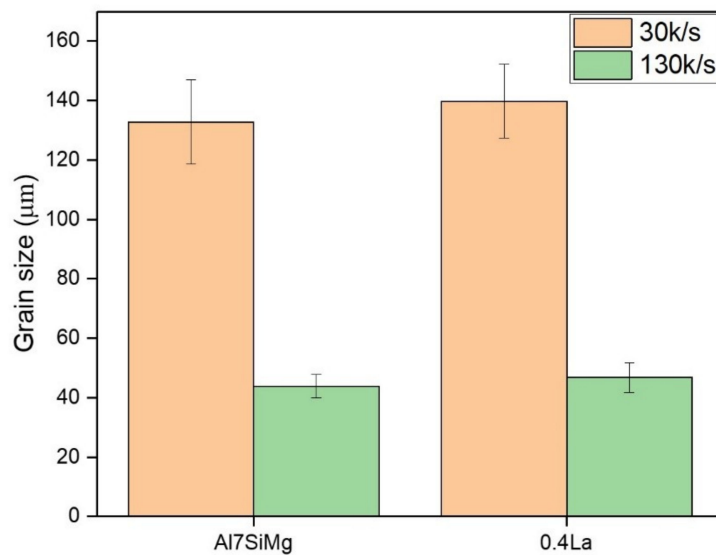
Figure 10. Measurement of α-Al grain size in Al7SiMg alloys without and with 0.4La at the cooling rates of 30 and 130 K/s.
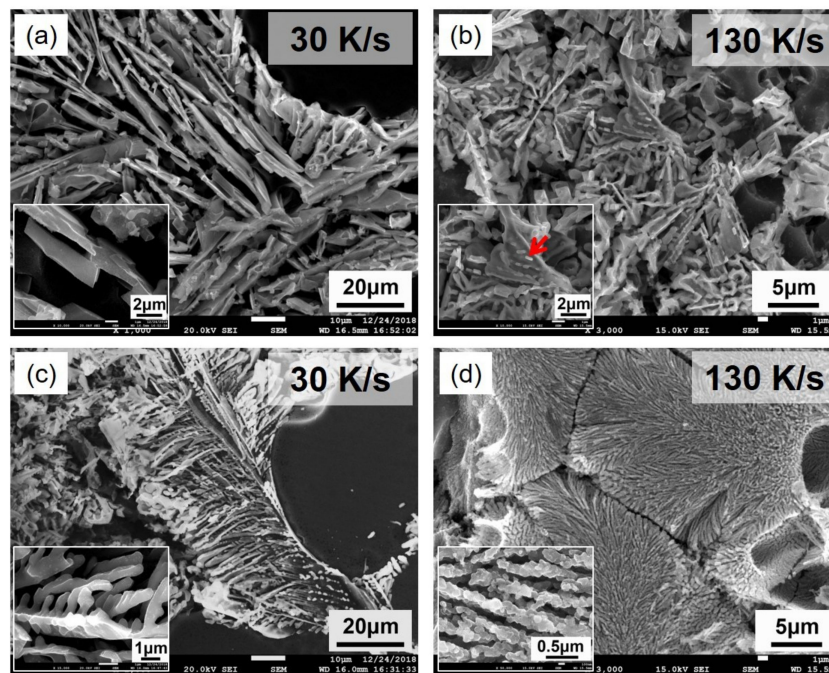
Figure 11. 3D morphology of eutectic Si in (**a**,**b**) Al7SiMg and (**c**,**d**) Al7SiMg + 0.4La alloys at the cooling rate of 30 and 130 K/s.

Figure 12 is the SEM microstructure showing the morphology of La-rich phases at the cooling rate of 30 and 130 K/s. It is observed that the La-rich phases have acicular morphology at the cooling rate of 30 K/s, while the La-rich phases have short rod-like structure with increasing the cooling rate to 130 K/s. Moreover, at high cooling rate (Figure 12b), the fine La-rich phases distribute in network way between the grain boundaries, and a large number of La-rich phases per unit area is obviously found. At high cooling rate, the microstructure including the α-Al grains and Si particles is well refined, as shown in Figures 9 and 11. The refined α-Al grains and Si particles result to an increasing number of gain boundaries per unit volume. Thus, the La-rich phases, which precipitate in grain boundaries, have more quantity per volume and smaller size at higher cooling rate. Moreover, the high cooling rate gives the La-rich phases less time to grow, thus the La-rich phases in small size form in microstructure.
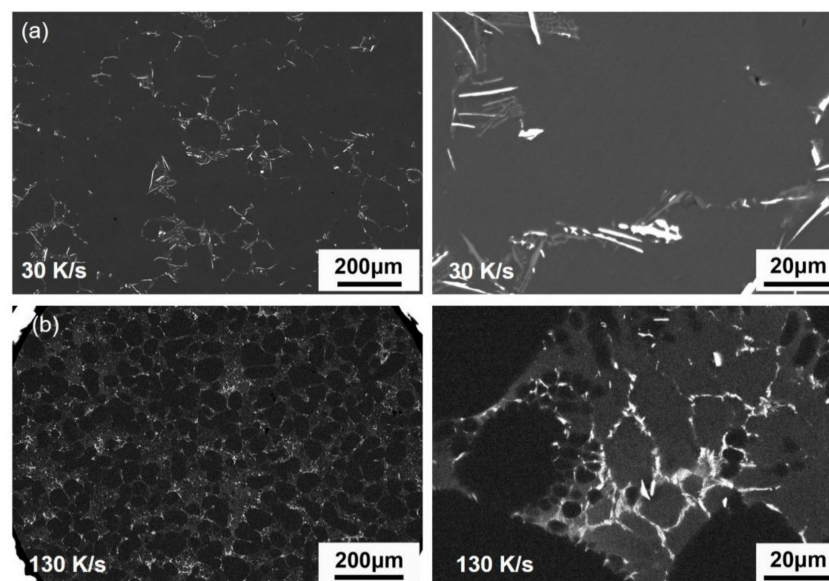
Figure 12. SEM microstructure showing the morphology of La-rich phases. (**a**) 30, (**b**) 130 K/s.

The tensile results are displayed in Table 3. It is obtained in Al7SiMg alloys that, when the cooling rate increases from 30 to 130 K/s, the UTS and elongation are increased from 200 to 230 MPa and 11% to 15%, respectively. Unlike the effect of La in gravity die casting, the addition of 0.4 wt.% La results to a slight decrease in strength and elongation of Al7SiMg alloys.

Table 3. Tensile properties of Al7SiMg and Al7SiMg + 0.4La alloys at different cooling rates. (YS = yield strength, UTS = ultimate tensile strength, EL = elongation).

Cooling Rate (K/s)	Alloys	YS (MPa)	UTS (MPa)	EL (%)
30 K/s	Al7SiMg	81 ± 2.3	200 ± 3.3	11 ± 1.5
	0.4 La	77 ± 2.3	190 ± 3.3	10 ± 0.8
130 K/s	Al7SiMg	100 ± 1.8	230 ± 5.8	15 ± 2.5
	0.4 La	100 ± 3.5	230 ± 2.4	11 ± 0.6

The microstructures of fracture at the cooling rate of 30 and 130 K/s are observed by SEM, as shown in Figure 13. It is found that the dimples are present on the fracture, which means the materials have good ductility. By increasing the cooling rate to 130 K/s, the α-Al grains and Si particles with fine morphology are observed in Figure 13b,d. No much difference can be observed between the Al7SiMg alloys and Al7SiMg alloys containing 0.4 wt.% La.
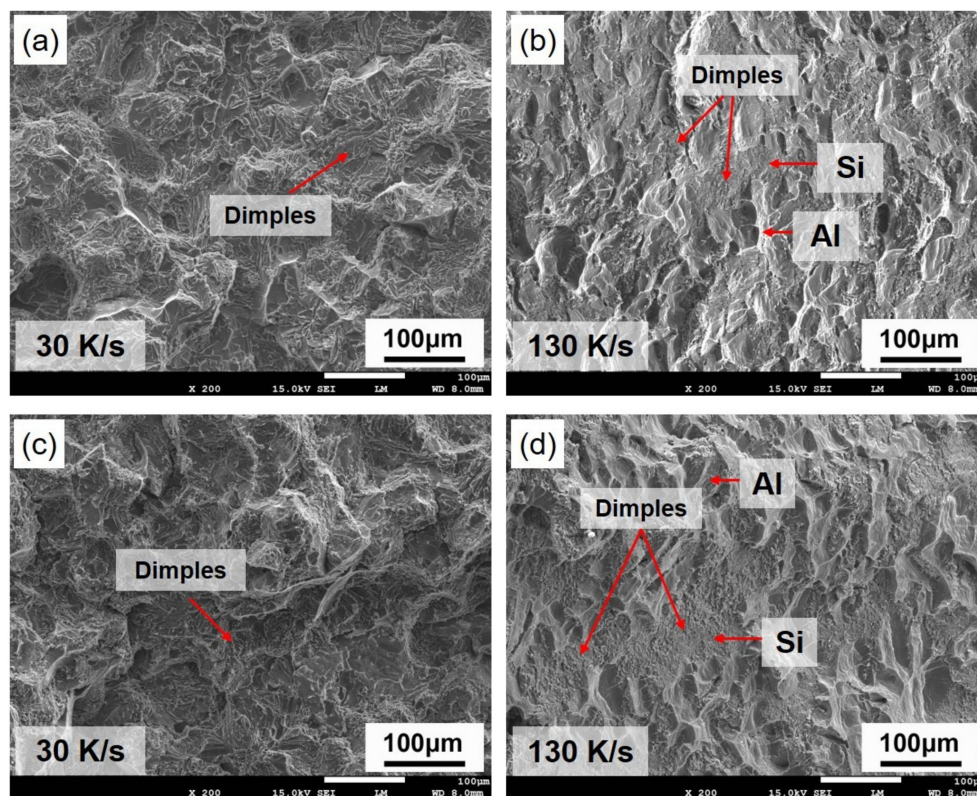
Figure 13. SEM pictures showing the fractures of (**a**,**b**) Al7SiMg and (**c**,**d**) Al7SiMg + 0.4La at the cooling rate of 30 and 130 K/s.

4. Discussion

In this part, the effect of cooling rates on microstructure and tensile properties of La modified Al7SiMg is discussed in the gravity die casting and semi-solid die casting. Figure 14 is the schematics showing the microstructural evolution of La modified Al7SiMg alloys in two casting processes. In gravity die casting (Figure 14a,b), due to the increase of cooling rate (0.2 to 9 K/s), a larger

undercooling is achieved and the process of nucleation in the melt is promoted [19,20], the grain size and DAS of α-Al phase are both refined. In addition, under 0.4 wt.% La additions, the Si modification effect of La is enhanced with increasing cooling rate. With the cooling rate increasing to 9 K/s, the Si particles are modified to branching morphology. During the tensile process, the cracks in materials play an important role. The fine Si particles can inhibit the initiation and propagation of the cracks, and decrease the stress concentration during tensile tests [21,22]. Therefore, the UTS and elongation of alloys are greatly enhanced.
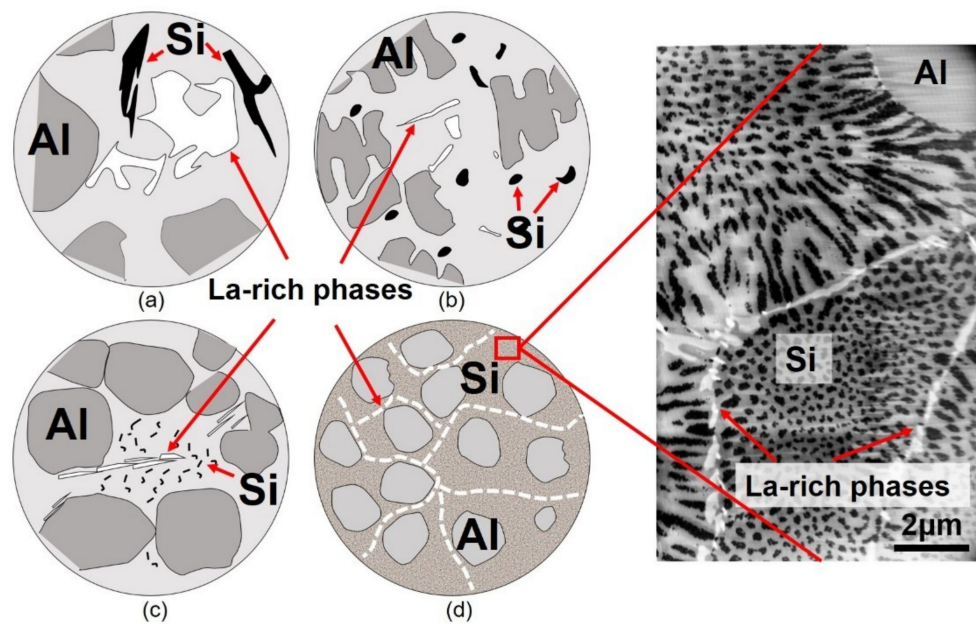
Figure 14. Schematics showing the microstructural evolution in La modified Al7SiMg alloys at the cooling rate of (**a**) 0.2 and (**b**) 9 K/s in the gravity die casting and (**c**) 30 and (**d**) 130 K/s in the semi-solid die casting.

In semi-solid die casting (Figure 14c,d), the globular α-Al grains are obtained at the cooling rate of 30 and 130 K/s. The sharp increase in cooling rate to 130 K/s results to finer α-Al grain size (about 50 µm). The grain refining supports the alloy a considerable enhancement in the strength. Moreover, the high cooling rate further promotes the Si modification effect of La. At high cooling rate, the growth velocity of Si crystals is significantly increased by increasing growth undercooling [23], which results to the increase of La solubility in Si. According to the IIT (impurity induced twinning) mechanism proposed by Lu and Hellawell [24], the modifier La, which has a favorable atomic size, is able to produce twins and stops the anisotropic growth of Si particles, and thus modifies the Si to fibrous morphology, as shown in the Figure 14d. The modification of eutectic Si enhances the UTS and elongation of alloys at high cooling rate. In addition, in the final stage of solidification, the La-rich phases are formed at the region of α-Al and Si grain boundaries. Different from the condition in gravity die casting, the refinement of α-Al grains and modification of Si particles are more obvious in semi-solid die casting. The decreasing size of α-Al grain and Si particles lead to an increasing number of grain boundaries per unit volume, which are the probable nucleation sites of La-rich phases. As shown in Figure 14d, an increasing number of La-rich phases happens at the cooling rate of 130 K/s, the La-rich phases in net shape distribution increase the stress concentration of materials. During the load process in tensile test, the stress transfers from α-Al grains, Si particles to La-rich phases, the La-rich phases become vulnerable part, which enhance the initiation and propagation of cracks, and thus decrease the strength and elongation of Al7SiMg alloys. From the above, at high cooling rate, the positive effect of fiber-like Si particles and negative effect of La-rich phases on the UTS and elongation are produced in alloys modified with La addition. An attempt of decreasing La content

in Al7SiMg alloys can be a method to decrease the quantity of La-rich phases and then improve the tensile properties in further study.

5. Conclusions

The influence of cooling rate on the microstructure and mechanical properties of Al7SiMg alloys with and without 0.4 wt.% La has been investigated in gravity die casting and semi-solid die casting. The conclusions are summarized as follow:

- The effect of grain refinement is greatly enhanced with increasing cooling rate in the gravity die casting, with increasing the cooling rate from 0.2 to 9 K/s, for Al7SiMg alloys, the DAS and grain size of α-Al phase are reduced from 106 to 19 μm and 1321 to 485 μm, respectively, which results to the enhancement of UTS from 140 to 160 MPa.
- With 0.4 wt.% La addition to Al7SiMg alloys in the gravity die casting, the modification effect of La is enhanced with increasing cooling rate. When the cooling rate increases from 0.2 to 9 K/s, the Si particles are modified from flake-like to branching morphology, which evidently increases the UTS from 140 to 190 MPa and elongation from 2.5% to 4.6%.
- In the semi-solid die casting, when increasing the cooling rate from 30 to 130 K/s, for Al7SiMg alloys, the globular α-Al grains are refined from 133 to 44 μm, the morphology of eutectic Si transfers from acicular to well-branching structure. The UTS and elongation of Al7SiMg alloys are increased from 200 to 230 MPa and 11% to 15%, respectively.
- When 0.4 wt.% La is added to Al7SiMg alloys in the semi-solid die casting, although the Si particles are modified to fibrous morphology, La-rich phases with a large number are formed in net shape distribution, which has no positive effect on the UTS and elongation of alloys.
- Compared to the microstructures in gravity die casting, the α-Al refinement effect and Si modification effect are greatly enhanced in the semi-solid die casting, which results to an obvious increase in the strength and elongation of alloys.

Author Contributions: Conceptualization, D.L.; Methodology, D.L.; Software, L.L.; Validation, L.L.; Formal analysis, J.F.; Investigation, L.L.; Resources, D.L.; Data curation, L.L.; Writing—Original draft preparation, L.L.; Writing—Review and editing, D.L., J.F., Y.Z., Y.K.; Visualization, L.L.; Supervision, D.L., Y.Z., Y.K.; Project administration, D.L.; Funding acquisition, D.L. All authors have read and agreed to the published version of the manuscript.

Conflicts of Interest: The authors declare no conflict of interest.

References

1. Polmear, I. *Light Alloys*, 4th ed.; Butterworth-Heinemann: Oxford, UK, 2005; pp. 220–226.
2. Campbell, J. *Castings*, 2nd ed.; Butterworth-Heinemann: Oxford, UK, 2003; pp. 205–210.
3. Hirsch, J. Recent development in aluminium for automotive applications. *Trans. Nonferrous Met. Soc. China* **2014**, *24*, 1995–2002. [CrossRef]
4. Kapranos, P. Current state of semi-solid net-shape die casting. *Metals* **2019**, *9*, 1301. [CrossRef]
5. Midson, S.P. Industrial applications for aluminum semi-solid castings. *Solid State Phenom.* **2014**, *217–218*, 487–495. [CrossRef]
6. Zhang, Y.H.; Ye, C.Y.; Shen, Y.P.; Chang, W.; StJohn, D.H.; Wang, G.; Zhai, Q.J. Grain refinement of hypoeutectic Al-7wt.%Si alloy induced by an Al–V–B master alloy. *J. Alloys Compd.* **2020**, *812*, 152022. [CrossRef]
7. Zamani, M.; Seifeddine, S. Determination of optimum Sr level for eutectic Si modification in Al–Si cast alloys using thermal analysis and tensile properties. *Int. J. Metalcast.* **2016**, *10*, 457–465. [CrossRef]
8. Riestra, M.; Ghassemali, E.; Bogdanoff, T.; Seifeddine, S. Interactive effects of grain refinement, eutectic modification and solidification rate on tensile properties of Al-10Si alloy. *Mater. Sci. Eng. A* **2017**, *703*, 270–279. [CrossRef]

9.   Moniri, S.; Shahani, A.J. Chemical modification of degenerate eutectics: A review of recent advances and current issues. *J. Mater. Sci.* **2019**, *34*, 20–34. [CrossRef]

10. Sigworth, G.K. The modification of Al-Si casting alloys: Important practical and theoretical aspects. *Int. J. Metalcast.* **2008**, *22*, 19–40. [CrossRef]

11. Kang, J.; Su, R.; Wu, D.Y.; Liu, C.H.; Li, T.; Wang, L.S.; Narayanaswamy, B. Synergistic effects of Ce and Mg on the microstructure and tensile properties of Al-7Si-0.3Mg-0.2Fe alloy. *J. Alloys Compd.* **2019**, *796*, 267–278. [CrossRef]

12. Pourbahari, B.; Emamy, M. Effects of La intermetallics on the structure and tensile properties of thin section gravity die-cast A357 Al alloy. *Mater. Des.* **2016**, *94*, 111–120. [CrossRef]

13. Mousavi, G.S.; Emamy, M.; Rassizadehghani, J. The effect of mischmetal and heat treatment on the microstructure and tensile properties of A357 Al–Si casting alloy. *Mater. Sci. Eng. A* **2012**, *556*, 573–581. [CrossRef]

14. Jiang, W.; Fan, Z.; Dai, Y.; Li, C. Effects of rare earth elements addition on microstructures, tensile properties and fractography of A357 alloy. *Mater. Sci. Eng. A* **2014**, *597*, 237–244. [CrossRef]

15. Mao, G.L.; Yan, H.; Zhu, C.C.; Wu, Z.; Gao, W.L. The varied mechanisms of yttrium (Y) modifying a hypoeutectic Al–Si alloy under conditions of different cooling rates. *J. Alloys Compd.* **2019**, *806*, 909–916. [CrossRef]

16. Liu, W.Y.; Xu, C.; Xiao, W.L.; Liu, M.W.; Zhang, J.B.; Chen, J.X.; Ma, C.L. Effects of cooling rate on morphology of eutectic Si in RE modified Al-10wt.%Si alloy. *Mater. Sci. Forum* **2016**, *850*, 587–593. [CrossRef]

17. Li, L.F.; Li, D.Q.; Mao, F.; Feng, J.; Zhang, Y.Z.; Kang, Y.L. Effect of cooling rate on eutectic Si in Al-7.0Si-0.3Mg alloys modified by La additions. *J. Alloys Compd.* **2020**, *826*, 154206. [CrossRef]

18. Langlais, J.; Lemieux, A. The SEED technology for semi-solid processing of aluminum alloys: A metallurgical and process overview. *Solid State Phenom.* **2006**, *116–117*, 472–477. [CrossRef]

19. Liang, G.F.; Ali, Y.; You, G.Q.; Zhang, M.X. Effect of cooling rate on grain refinement of cast aluminium alloys. *Materialia* **2018**, *3*, 113–121. [CrossRef]

20. Guan, T.; Zhang, Z.; Bai, Y.; Li, B.; Wang, P. Enhanced Refinement of Al-Zn-Mg-Cu-Zr Alloy via Internal Cooling with Annular Electromagnetic Stirring above the Liquidus Temperature. *Materials* **2019**, *12*, 337. [CrossRef]

21. Mao, F.; Chen, F.; Yan, G.; Wang, T.; Cao, Z. Effect of strontium addition on silicon phase and mechanical properties of Zn–27Al–3Si alloy. *J. Alloys Compd.* **2015**, *622*, 871–879. [CrossRef]

22. Mao, F.; Yan, G.Y.; Xuan, Z.J.; Cao, Z.Q.; Wang, T.M. Effect of Eu addition on the microstructures and mechanical properties of A356 aluminum alloys. *J. Alloys Compd.* **2015**, *650*, 896–906. [CrossRef]

23. Hosch, T.; England, L.G.; Napolitano, R.E. Analysis of the high growth-rate transition in Al–Si eutectic solidification. *J. Mater. Sci.* **2009**, *44*, 4892–4899. [CrossRef]

24. Lu, S.Z.; Hellawell, A. The mechanism of silicon modification in Aluminum-Silicon alloys: Impurity induced twinning. *Metall. Mater. Trans. A* **1987**, *18*, 1721–1733. [CrossRef]